

# An Ultrasonic Global Inspection Technique for an Offshore K-Joint

J.L. Rose, Drexel U.  
M.C. Fuller, Drexel U.  
J.B. Nestleroth, Drexel U.  
Y.H. Jeong, Drexel U.

## Abstract

The catastrophic collapse of several offshore platforms has spurred the development of nondestructive inspection techniques for offshore structures. Presented here are the concepts of an ultrasonic global inspection technique. Also presented are the results of feasibility studies conducted on  $1/9$ -,  $1/10$ -, and  $1/2$ -scale model K-joint models using this technique for early detection of damage. The technique takes advantage of the geometry of tubular joints to give global ultrasonic coverage of a joint while employing a similarity-coefficient-based algorithm for actual damage detection. The data from the scaled models indicate a correlation between the value of the similarity coefficient and the extent of induced damage. The results are encouraging for further development of the technique for field use.

## Introduction

The integrity of the supporting steel structure of offshore platforms is of universal concern, both to industry and to associated regulatory administrations.<sup>1,2</sup> Failure of support structures is extremely costly in money and in lives. The U.S. Minerals Management Service, charged with ensuring safe oil and gas operation on the outer continental shelf, has actively supported the research and development of means to ensure the integrity of such offshore structures. As part of these funded activities, Drexel U. has pursued the research and development of a new ultrasonic inspection technique for the early detection of damage to large tubular K-joints. Because of its generic

nature, this technique also is applicable to other structural joints often found in tubular casings.

The goal is to develop an inspection technique that will successfully monitor the health of an entire joint and that will provide an indication of accumulated damage. Thus, it is desirable to develop a global inspection technique that will monitor a large area of a structure, in preference to a traditional ultrasonic technique that can address itself only to very localized areas of a structure. Therefore, the problem is simply to develop a procedure that will consistently reflect the onset and accumulation of damage, regardless of its location in the joint, using a minimum amount of equipment and inspection time.

To ensure global coverage and to ensure the proper design and selection of equipment, it was necessary to study the propagational behavior of sound energy in tubular sections. This was effected in part by studying three scaled models ( $1/9$ ,  $1/10$ ,  $1/2$ ) of a K-joint structure. Side-drilled holes were introduced in the  $1/9$ -scale model and saw cuts in the  $1/10$ -scale model. Actual cracks were introduced in the  $1/2$ -scale model. Consideration of the effects of this damage on the propagation of ultrasonic energy, along with other physically constraining factors, led to the development of a suitable inspection technique.

As a result of these studies, a microprocessor-based inspection system has been developed<sup>3-5</sup> (Fig. 1) using a low-frequency through-transmission technique and a damage-detection algorithm based on a similarity-coefficient concept (a statistical correlation). The factors affecting the global inspection technique (using the

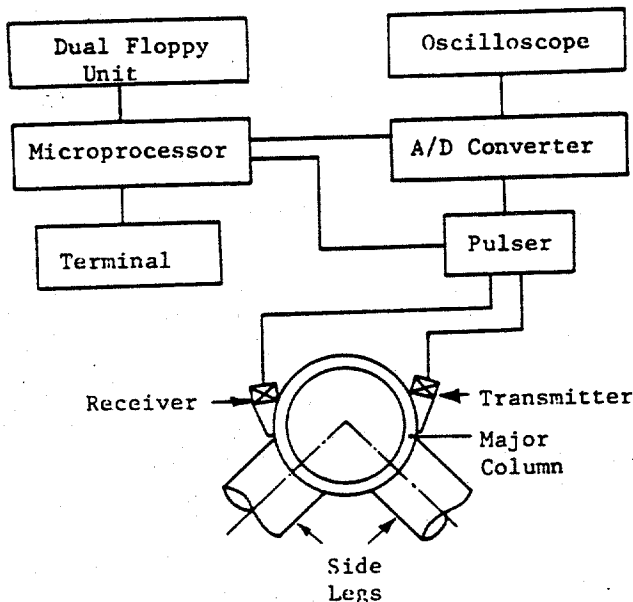


Fig. 1—Microprocessor-based inspection system for tubular joints.

similarity coefficient) are presented here along with the results obtained from applying this technique to the variously scaled models of the K-joint.

### The Global Inspection System

Conventional ultrasonic inspection techniques generally employ high-frequency ultrasonic wave propagation applied to very local areas; thus, flaw detection traditionally involves some type of scanning. The goal was to develop a new technique, one in which the health of an entire structural joint could be monitored without the benefit of divers or probe manipulation. A feasibility study was conducted using scaled models to validate the inspection procedure devised.

The immense size of offshore platforms presents a formidable challenge to the implementation of any practical ultrasonic technique. The primary concern is signal attenuation. Energy must be transmitted around the circumference of the casing, which in the full-scale case is on the order of 4.28 m. The distance that sound must travel, or the sound-path distance, becomes important. This plus the requirement that the entire joint must be monitored are the design conditions that must be considered.

As a result of a series of studies on attenuation and wave transmission, the transducer system shown in Fig. 2 was selected for use in this program. The transducers were placed as close to the inspection zone as is practical to minimize the sound-path distance. In addition, because of the inherently longer sound paths associated with pulse echo, a through-transmission design was selected. The selection of the angle  $\theta$  (shown in Fig. 2) and the frequency of the transducers is a function of the

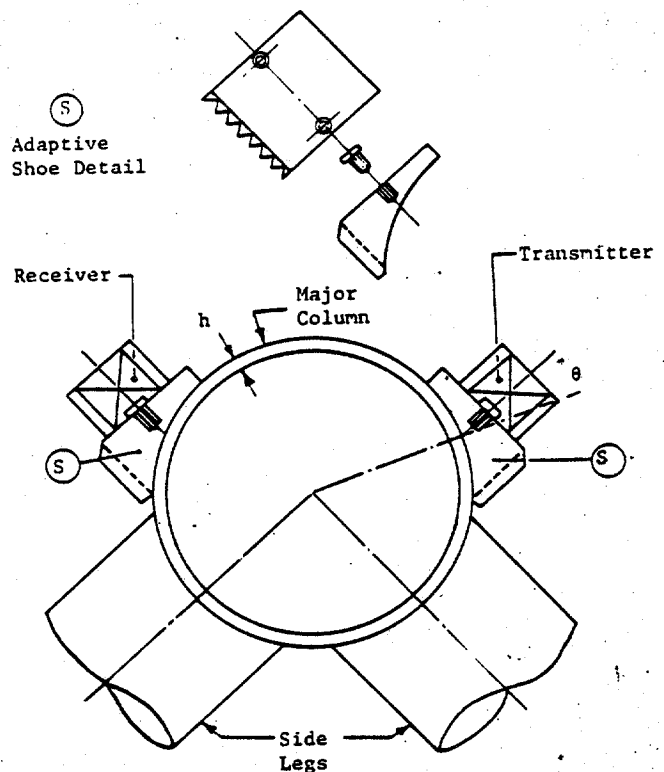


Fig. 2—Transducer configuration for global inspection system.

wall thickness,  $h$ . Basically, the goal is to select values of  $\theta$  and  $f$  that will excite a Lamb wave in the casing, while maintaining a low-enough frequency value to ensure that the ultrasonic signal is not attenuated excessively.

The Lamb-wave excitation concept provides the basis for the global inspection concept. Within a short distance of the transmitter, the entire thickness of the casing is flooded with ultrasonic energy, the walls acting as wave guides. Therefore, if damage occurs anywhere between the transducers (in the inspection zone), it should be detectable without scanning or probe manipulation.

The information obtained from the receiving transducer appears as a signal in the form shown in Fig. 3A. Any physical damages that may occur in the inspection zone will influence the ultrasonic field, thereby creating an interference phenomenon and altering the received signal, qualitatively shown in Fig. 3B. This change in signal, when quantified, becomes the key to detecting damage.

A statistical measure used for the comparison of signals and a quantification of their differences is called a similarity coefficient. By utilizing total ultrasonic coverage and by monitoring this single indicator — the similarity coefficient — damage may be detected.

The concept and functional relationships governing the attenuation of energy and the excitement of Lamb waves are reviewed next.

The attenuation of ultrasonic energy is governed by the following equation.

$$p = p_0 \pi \left( \frac{d_t - \lambda}{4L_s \lambda} \right) e^{-\alpha L_s}, \dots \dots \dots (1)$$

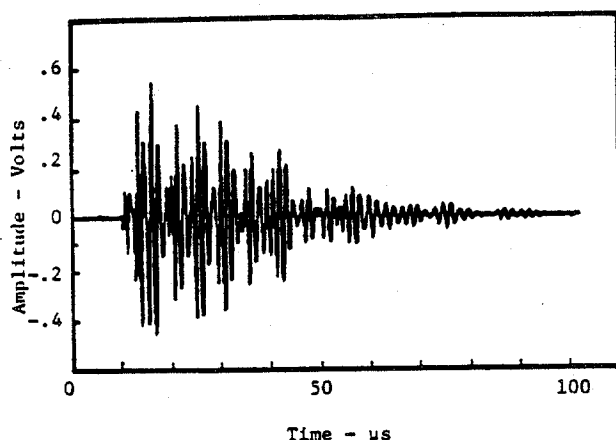


Fig. 3A—Ultrasonic waveform obtained from undamaged joint.

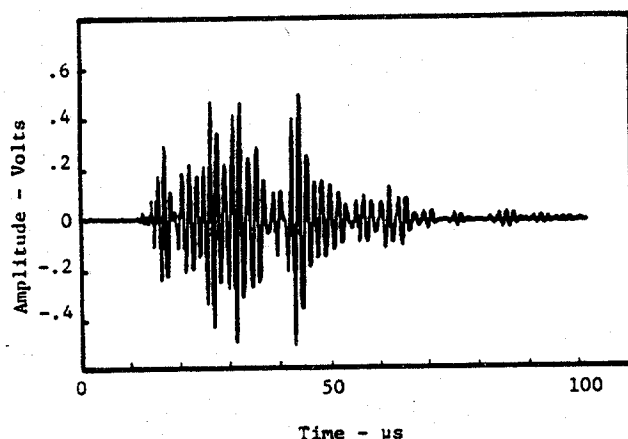


Fig. 3B—Ultrasonic waveform obtained from joint after sustaining damage.

where

$p$  = sound pressure,  
 $d_t$  = transducer diameter,  
 $L_s$  = distance from probe, and  
 $\alpha$  = attenuation coefficient.

It is important to note that

$$\alpha \sim f \left( \frac{G}{\lambda} \right)^3, \dots \dots \dots (2)$$

where  $G$  is the characteristic grain size of the material being inspected, and  $\lambda$  is the wavelength of the ultrasonic wave.

As can be seen from these two equations, the attenuation of energy is tremendously affected by sound path distance,  $L_s$ , and the ultrasonic wavelength,  $\lambda$ .

The wavelength affects not only the attenuation coefficient,  $\alpha$ , but also the divergence of the ultrasonic beam. Beam divergence has two effects on the inspection of thin wall casings; first, it has an attenuative effect, roughly inversely proportional to the distance from the probe as seen in Eq. 1, and second, it excites the propagation of the Lamb waves.

The generation of Lamb waves can be considered to occur as the width of the beam becomes larger than the

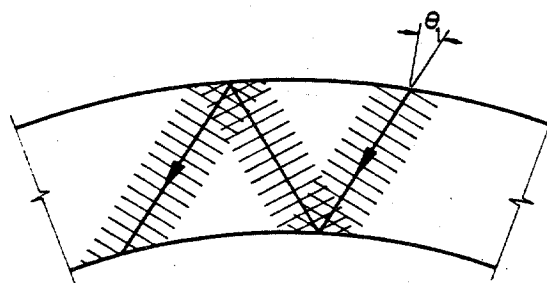


Fig. 4A—Traditional high-frequency ultrasonic wave propagation.

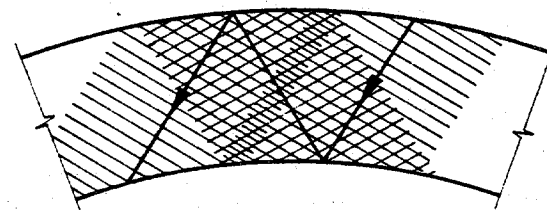


Fig. 4B—Unfavorable interference at low frequency resulting from improper value of  $\theta_1$ .

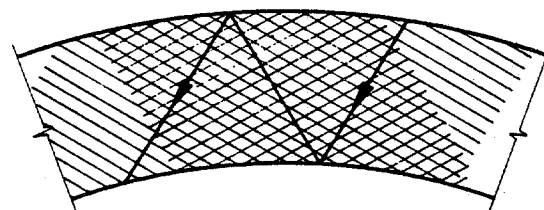


Fig. 4C—Lamb-wave propagation resulting from favorable interferences of reflecting wave fronts (proper choice of  $\theta_1$ ).

width of the casing (dictated by the angle of divergence). As this occurs, the reflections from various skips will begin to overlap and hence to interfere (Fig. 4). According to Lamb and others,<sup>6,7</sup> favorable wave propagation will occur when the phase positioning of the beams (dictated by  $\theta$ ) is constructive (Fig. 4C). Thus, in reality there is a complex wave propagation, composed of both longitudinal and shear waves, continuously mode converting and traveling in a more or less zigzag fashion. Thus, as seen in Fig. 4C, the walls of the casing guide the plate wave, while the material within is totally bathed in ultrasound, allowing total surveillance of the tubing.

The relationship between casing thickness, angle, and wavelength  $\lambda$  for successful excitation of Lamb waves has been determined by Redwood.<sup>8,9</sup> Thus, the transducers are designed by selecting the optimal frequency and angle  $\theta$  so that a plate wave is excited while maintaining the proper value of the frequency to ensure that energy at the receiver is of a satisfactory level.

### Similarity-Coefficient Analysis

The application of the similarity coefficient is a new concept in ultrasonic evaluation of materials. This section outlines the character of the technique as well as the specifics of its application.

The similarity-coefficient analysis is the key to detecting damage. The similarity coefficient is primarily a statistical correlation technique that allows the comparison of any two conformable vectors. The vectors in this case are two ultrasonic waveforms (in digital form), one from a reference or good state and the other taken from a structure whose integrity is in question. Since damage will alter the waveform of the received signal, a high correlation would not be expected. The similarity coefficient, as used in this application, may vary from zero to one (a similarity of one being associated with two totally identical signals). Thus, the detection of damage may be correlated with a drop in the value of the similarity coefficient as indicated by the experimental results.

In applying the similarity-coefficient analysis in the field, it was desirable to desensitize the analysis to certain external variables, effects that could easily influence this type of correlation technique and therefore give false indications of damage. Arrival time and amplitude variations can and do arise easily from the variations in transducer placement (shorter or longer sound-path distances). The effects of these variations on the similarity coefficient could be large and perhaps outweigh the effects caused by damages.

If the Fourier transform of the data is taken before applying the similarity-coefficient measure, the effects of amplitude and arrival-time variations may be eliminated. If the power spectra of two signals are compared in lieu of their time-domain inverses, it is possible to eliminate the effects of signal amplitude. This is because the power spectrum is a probability-density function; these functions are always area-normalized before any further manipulation. In addition, the effects of an arrival-time difference or phase shift are eliminated as follows.

Consider a signal given by  $f(t)$  and a second by  $f(t-T)$  where  $T$  is the phase shift. This is the ideal case when the signals are identical but displaced in time relative to each other. Taking the Fourier transform of each gives

$$\mathcal{F}[f(t-T)] = e^{-j\omega T} F(\omega) \quad (3)$$

and

$$\mathcal{F}[f(t)] = F(\omega) \quad (4)$$

Now the power spectrum of each is given by  $|F(\omega)|^2$ , since

$$[e^{-j\omega T} F(\omega)] \times [e^{j\omega T} F(\omega)^*] = |F(\omega)|^2 \quad (5)$$

Thus the power spectra are identical, and the effects of the time delay are removed.

The formulation of the similarity coefficient is given as follows.<sup>10</sup>

$$s(\vec{x}, \vec{y}) = \frac{\vec{x}'\vec{y}}{\vec{x}'\vec{x} + \vec{y}'\vec{y} - \vec{x}'\vec{y}} \quad (6)$$

where

$\vec{x}$  = a digital representation of a reference (before damage) ultrasonic waveform (a vector),

$\vec{y}$  = a digital representation of an ultrasonic waveform obtained for comparison (a vector),

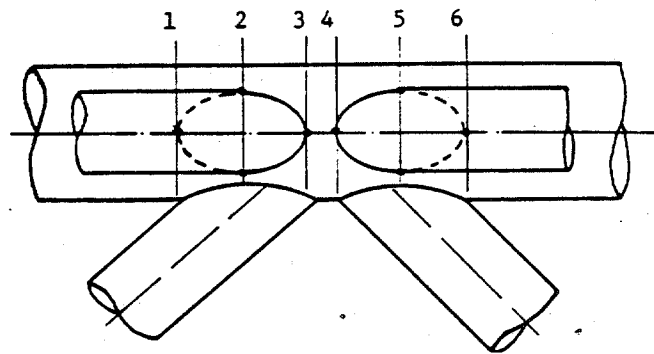


Fig. 5—Data acquisition locations for 1/19-scale model testing; • indicates damages induced by side-drilled holes.

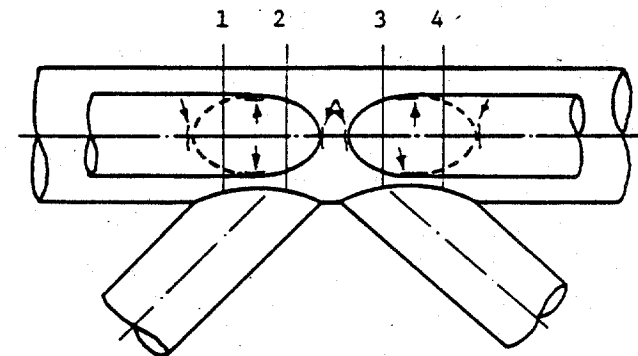


Fig. 6—Data acquisition locations for 1/10-scale model testing; arrows denote damage induced by saw cuts.

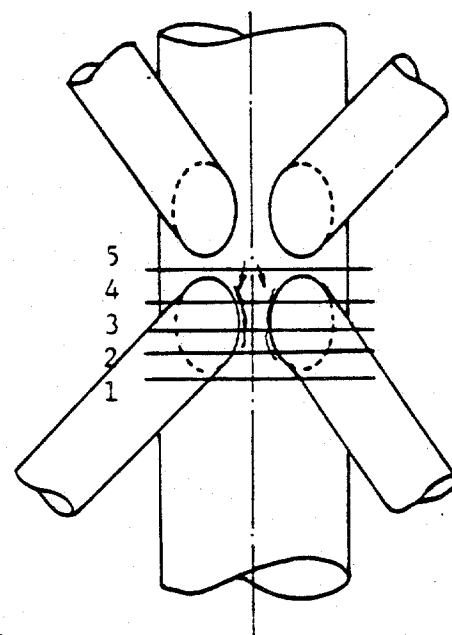
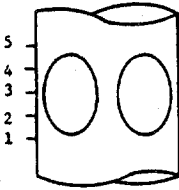
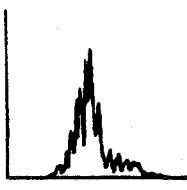
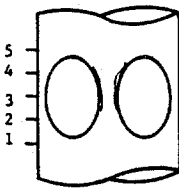
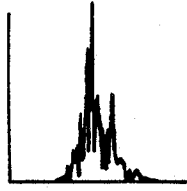


Fig. 7—Data acquisition locations for 1/3-scale model K-joint; arrows indicate damage.

Damage Status	Visual Identification	Crack Length (mm)		Power Spectrum†	Overall Similarity†
		Left	Right		
A*		0	0		.954
B**		254	279		.638

\*No damage.

\*\*Damage, crack detected 100% through major column thickness on right side.

†These data from Transducer Position 4.

Fig. 8—Damage status for 1/3-scale model K-joint.

$t$  = the vector transpose, and  
 $s(\vec{x}, \vec{y})$  = the similarity coefficient between the two vectors  $x$  and  $y$ .

Recall that the ultrasonic waveforms are in the frequency domain. Since all values of the power spectrum are positive,  $s(\vec{x}, \vec{y})$  will always be positive. Note that if  $\vec{y} = \vec{x}$ , then  $s(\vec{x}, \vec{y}) = 1$ , which is its maximum value. If  $\vec{y} = 0$  (total rupture), then  $s(\vec{x}, \vec{y}) = 0$ , which is the minimum value and shows the complete dissimilarity of the vectors.

There are several weighting and windowing techniques that may be employed in a similarity analysis to increase the sensitivity of the technique to specific portions of the spectrum. In this fashion, anomalies in the power spectra that are ordinarily undetectable may now be quantified. Specifically, in the damage analysis of tubular joints, the power spectra of reference and comparison signals were windowed in quarters about the center frequency of the signal. By doing this, the data have shown that the detection of damage may be more sensitive but somewhat noisier.

## Experimental Results

The employment of the similarity coefficient for the assessment of damage in variously scaled models of the K-joint established the following protocol. The transducers were placed on the undamaged model, and ultrasonic energy was pulsed into the inspection zone at a repetition rate of approximately 800 kHz. The transducers used depended on the plate thickness of the model. The data-acquisition system shown in Fig. 1 was used to average and to store a reference signal digitally. Damage was then inflicted on the models, so an average of the ultrasonic signal was again acquired and stored. A fast Fourier transform was performed on all data files, and similarity coefficients were calculated between the

reference data and data representative of various degrees of inflicted damage. The specific experiments and the results are presented next.

Experiments utilizing the global inspection technique previously described were conducted on 1/9-, 1/10-, and 1/3-scale models of a K-joint. While artificial damage was inflicted on the 1/9- and 1/10-scale models, the 1/3-scale model sustained damage of a much more realistic nature—i.e., actual cracks.

Two 1/9-scale K-joint models were fabricated at Drexel U. The global signals from six different locations were acquired using a set of 2.25-MHz transducers. The data-acquisition locations are shown in Fig. 5 and the orientation of the transducers were shown in Fig. 2.

The signals without damage were acquired from each location and used as reference signals. For the flaw simulation, side-drilled holes starting from 1.59 mm in diameter were machined in 0.40-mm increments. Ultrasonic signals were obtained from each machining step, digitally stored, and the similarity coefficient was calculated.

As a result of this study, it was found that the technique (in this scaling exercise) was not sensitive to damage less severe than that corresponding to a 2.38-mm side-drilled hole. At this point, a distinct drop in the value of the similarity coefficient to 0.8 was observed. A 2.38-mm hole corresponds to 1.2% of the total weld length.

In addition to the 1/9-scale models, two 1/10-scale K-joint models were also fabricated. Under the design criteria presented earlier, a set of 1-MHz transducers was selected for this experiment. Data were acquired from four locations (Fig. 6). Damages on the K-joint welds were generated by saw cuts, starting from 12.7 mm in length in 3.17-mm increments. Again, the similarity analysis was carried out.

As a result of this study, it was found that a 38.1-mm saw cut could be detected and was accompanied by a drop in the similarity coefficient to a value of 0.7. A saw cut of this size represents 12% of the total weld length on the  $\frac{1}{10}$ -scale model.

A final set of experiments was conducted on a  $\frac{1}{10}$ -scale model constructed by the U. of Maryland. For this experiment, a set of 800-kHz transducers was specially manufactured (they are not commercially available), and five transducer locations were selected (Fig. 7). The test protocol for this experiment is similar to that of the previous experiments. Fig. 8 shows the extent of the induced damage at successive transducer locations; in addition, it shows the value of the similarity coefficient at Transducer Location 4, the most sensitive position. Fig. 9A shows the reference waveform and its Fourier transform for Transducer Location 4. In Fig. 9B, the waveform and Fourier transform for Data Point 2 is shown for comparison. Note that the time-domain signals are quite different. The difference becomes even more apparent when comparing spectral data. The value of the similarity coefficient for this particular comparison is 0.638. Table 1 shows the similarity values associated with various transducer locations. In addition, the power spectrum was windowed, splitting the data into quarters to improve the sensitivity of the technique to effects that may be present in a relatively narrow frequency range; these data are also shown in Table 1.

Fig. 8 shows that damage is primarily restricted to areas directly opposing Transducer Location 3 (Zone 3) and Transducer Location 4 (Zone 4).

The damage never entered areas that oppose Transducer Locations 1, 2, or 5. The overall similarity data in Table 1 indicate that damages are detected in both Zones 3 and 4, while no damage detection is apparent in Zones 1, 2, and 5.

A consideration of the data associated with the quarters of the spectrum that contain frequencies higher than the peak frequency indicates an increase in the sensitivity of the similarity coefficient to damage. This should be considered with care, however, since the analysis is being conducted on portions of the spectrum that contain relatively low energies. Thus, the influences of small effects may be pronounced, causing greater variations in the data.

The overall similarity data from Positions 1, 2, and 5 appear to indicate that the technique is relatively insensitive to damage that is not in a zone directly opposing the transducer location; however, the fourth spectral quarter (higher frequencies) may show some sensitivity to off-axis damage. Sensitivity to off-axis damage is currently being investigated.

## Conclusions

As a result of this study on tubular joint inspection, it has been determined that a similarity coefficient may be correlated to damage in a tubular structure. The data indicate that the technique is sensitive to damage in a zone relatively close to the axis of a particular receiving transducer. The data also indicate that the sensitivity to off-axis damage may be increased by examining specific portions of the spectrum. However, because of the instability of the signal in these lower energy portions, this cannot be stated conclusively without further study.

TABLE 1—SIMILARITY COEFFICIENT ANALYSIS FOR  $\frac{1}{10}$ -SCALE K-JOINT MODEL

Transducer Location	Damage Status	Overall	Similarity Coefficient			
			Spectral Quarter			
			1	2	3	4
1	A	0.943	0.885	0.955	0.957	0.982
1	B	0.924	0.881	0.935	0.968	0.543
2	A	0.973	0.941	0.981	0.972	0.921
2	B	0.947	0.895	0.963	0.930	0.498
3	A	0.912	0.829	0.953	0.720	0.646
3	B	0.667	0.549	0.740	0.503	0.260
4	A	0.954	0.874	0.968	0.934	0.988
4	B	0.638	0.831	0.597	0.701	0.246
5	A	0.958	0.958	0.960	0.955	0.916
5	B	0.859	0.775	0.886	0.839	0.408

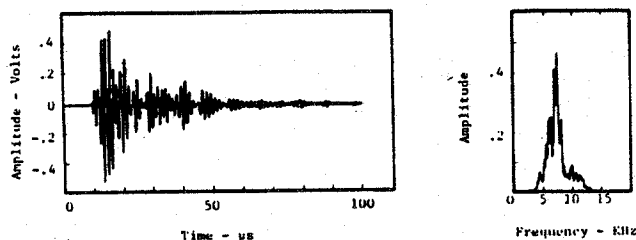


Fig. 9A—Ultrasonic waveform and its power spectrum obtained from 1/3-scale model K-joint containing no damage.

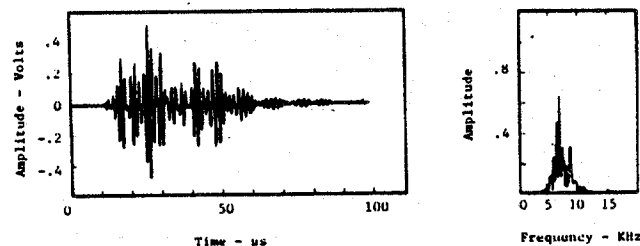


Fig. 9B—Ultrasonic waveform and its power spectrum obtained from 1/3-scale model K-joint after sustaining substantial damage. The value of the similarity coefficient for these signals is 0.658.

The inspection concept depends on the principle that damage may be detected anywhere in a zone between a set of transducers. This was realized by exciting Lamb waves in the structure. This global coverage depends heavily on the frequency of the probes used and their angle to the radius of the tube. Careful consideration of these parameters must be given to the design of the transducer system to excite a plate wave properly. Given the data obtained, it may be concluded that the use of higher frequencies is desirable for increased sensitivity, while the upper-frequency limit is dominated by the attenuation of the ultrasonic energy in the tubing. It is possible to design the probe angle for global coverage for any practical range of frequencies. Given these requirements, the optimal frequency for inspecting full-scale joints should be 500 to 800 kHz.

The data obtained during this study are encouraging and indicate that further development could yield a practical inspection procedure. The following areas remain to

be considered.

1. The optimal transducer locations must be determined to minimize the number of transducers needed for full inspection of a joint.

2. The sensitivity of the technique to off-axis damage must be studied. This includes investigating the stability of lower-energy portions of the spectrum.

3. The performance of the technique in a marine environment must be considered; this includes the effects of immersion and marine growth.

4. Before this technique may be field tested, permanent transducer placement must be considered in addition to overcoming the problem of transmitting subsurface data by cable or telemetry to an on-deck monitoring system.

Scaled model studies have shown the feasibility of a similarity-coefficient-based analysis. While  $1/10$ - and  $1/50$ -scale model data indicate that damage detection is possible, the  $1/3$ -scale model data show practical promise. The damages in the  $1/3$ -scale study are realistic—i.e., cracks—and the similarity coefficient correlates well. While windowing of the spectrum tends to increase sensitivity for the informed inspector, the field of view of this technique seems to be somewhat narrow, although there are indications that higher frequencies may improve this situation.

## Acknowledgments

The authors thank the Office of Naval Research and the U.S. Minerals Management Service (formerly U.S. Geol. Survey) for support on this project. Thanks also are extended to Michael J. Avioli for discussions and assistance on this effort.

## Nomenclature

- $d_t$  = transducer diameter
- $e$  = base of natural logarithm
- $f$  = transducer frequency
- $f( )$  = function of quantities in parenthesis
- $\mathcal{F}( )$  = indicates the Fourier transform
- $F(\omega)$  = Fourier transform of  $f(t)$
- $F(\omega)^*$  = complex conjugate of  $F(\omega)$
- $G$  = characteristic grain size
- $h$  = pipe wall thickness
- $j = \sqrt{-1}$
- $L_s$  = sound-path distance
- $p$  = sound pressure
- $p_o$  = sound pressure at a reference point
- $s(\vec{x}, \vec{y})$  = similarity coefficient between two vectors  $\vec{x}$  and  $\vec{y}$

$t$  = time variable

$T$  = phase shift

$\vec{x}$  = vector containing ultrasonic reference data

$\vec{x}'$  = transpose of vector  $\vec{x}$

$\vec{y}$  = vector containing ultrasonic data at some variable time

$\vec{y}'$  = transpose of vector  $\vec{y}$

$\alpha$  = ultrasonic attenuation coefficient

$\theta$  = transducer angle of incidence to the radius of the pipe

$\theta_1$  = angle of sound beam in plate to radius of pipe, related to  $\theta$  by Snells law

$\lambda$  = ultrasonic wavelength

$\pi$  = irrational number Pi

$\tau$  = finite time delay

$\omega$  = frequency variable

## References

1. *Outer Continental Shelf Oil and Gas Operations*, Technical Report 1981. John B. Gregory and Charles E. Smith (eds.), U.S. Geological Survey, Open-File Report 81-704 (1981) 1-42.
2. Smart, J.S. III: "Corrosion Failure of Offshore Steel Platforms," *Materials Performance*, (May 1980) 19, 5, 41-48.
3. Rose, J.L., Nestleroth, J.B., and Poplawski, E.G.: "Flaw Classification in Welded Plates Using a Microprocessor Controlled Flaw Detector," *NDT Intl.* (Aug. 1980) 159-64.
4. Rose, J.L., Nestleroth, J.B., and Jeong, Y.H.: "Component Identification Using Ultrasonic Signature Analysis," to be published in *Materials Evaluation*.
5. Rose, J.L.: "A Feature Based Ultrasonic System for Reflector Classification," *Proc.*, the German-American Workshop on Research and Development on New Procedures in Nondestructive Testing, Springer-Verlag, New York City (1982).
6. Lamb, H.: "On Waves in an Elastic Plate," *Proc.*, Royal Society of London (1916) A93, 114.
7. Krautkramer, J. et al.: *Ultrasonic Testing of Materials*, second edition, Springer-Verlag Inc., New York City (1969) 39.
8. Redwood, M.: "Ultrasonic Waveguides — A Physical Approach," *Ultrasonics* (April-June 1963) 99-105.
9. Redwood, M.: *Mechanical Waveguides*, Pergamon Press, London (1960) 208.
10. Duda, R.O. and Hart, P.E.: *Pattern Classification and Scene Analysis*, John Wiley and Sons Inc., New York City (1973) 213.

## SI Metric Conversion Factors

$$\begin{aligned} \text{cycle/sec} \times 1.000^* \text{ E}+00 &= \text{Hz} \\ \text{in.} \times 2.54^* \text{ E}+01 &= \text{mm} \end{aligned}$$

\*Conversion factor is exact.

SPEJ

Original manuscript received in Society of Petroleum Engineers office May 1, 1981. Paper accepted for publication Feb. 12, 1982. Revised manuscript received Nov. 23, 1982.